Asian Journal of Chemistry; Vol. 23, No. 12 (2011), 5577-5580

ASIAN JOURNAL OF CHEMISTRY

www.asianjournalofchemistry.co.in

Tailoring of Structural and Optical Properties of ZnO Nanoparticles by Co Doping†

MOHD ARSHAD[1,*], AMEER AZAM[2], ARHAM S. AHMED[1], S. MOLLAH[3] and ALIM H. NAQVI[1]

[1]Centre of Excellence in Materials Science (Nanomaterials), Department of Applied Physics, Aligarh Muslim University, Aligarh-202 002, India
[2]Centre of Nanotechnology, King Abdul Aziz University, Jeddah, Saudi Arabia
[3]Department of Physics, Aligarh Muslim University, Aligarh-202 002, India

*Corresponding author: E-mail: arshad_632000@yahoo.com

AJC-10335

Pure and Co doped ZnO nanoparticles have been synthesized by wet chemical route and characterized by X-ray diffraction (XRD), scanning electron microscopy (SEM), transmission electron microscopy (TEM), energy dispersive X-ray analysis (EDAX), UV-visible absorption spectroscopy and Fourier transform infrared spectroscopy (FTIR). X-ray diffraction analysis revealed the formation of single phase structure of all samples which was further supported by FTIR data. Crystallite size observed 27.1 for 0 % and 21.3 nm for 5 % Co concentration, suggesting the prevention of crystal growth with Co doping. It was clear from the absorption spectra that the absorbance tends to increase with the increase in dopant concentration. Optical band gap was calculated using Tauc relation and found to increase slightly with the increase in Co contents, confirming the size reduction as a result of Co doping.

Key Words: ZnO, Wet chemical, XRD, TEM, EDAX, FTIR.

INTRODUCTION

Zinc oxide (ZnO) is an excellent *n*-type semiconductor with a wide band gap of 3.37 eV and a large exciton binding energy of 60 meV[1,2]. For these reasons, ZnO is used in a wide variety of applications, including opto-electronic devices[3-6] catalysis[7], light-emitting diodes[8], thermoelectric devices[9], varistors[10,11], flat panel displays[11] and surface acoustic wave devices[12]. Recent theoretical predictions[13-18] proposed transition metal-doped ZnO as one of the most promising candidates for room-temperature ferromagnetism (RTFM). Additionally, the excellent optical transparency of ZnO and the possibility of band gap engineering through transition metal doping strongly encourage the exploration of the magneto-optical properties of the transition metal-doped ZnO system[19,20], which might lead to the development of novel magneto-optic electronic devices[21-23].

Zinc oxide nanoparticles also have a variety of applications such as UV absorption, deodorization and antibacterial treatment[24-26]. Several methods are reported in literature for the synthesis of doped and undoped ZnO nanoparticles which can be categorized either chemical or physical methods[27,28]. The chemical methods comprise thermal hydrolysis technique[29], hydrothermal processing[30] and sol-gel method[31-33] while the physical methods are vapour condensation method[34], spray pyrolysis[35-37] and thermo-chemical/flame decomposition of metal-organic precursors[38,39]. Wet chemical technique is being extensively used for synthesis of advanced ceramics, production of nanocrystalline materials and for metallurgical treatment of ores and minerals to yield value-added materials. Wet chemical method is easy to produce relatively large quantities of nanoparticles at low cost.

In the present investigation, we have studied structural and optical properties of Co-doped ZnO nanoparticles using XRD, SEM, TEM, EDAX, UV-Visible and FTIR spectroscopies.

We have adopted here a procedure in this respect where Co-doped ZnO nanoparticles with 25 nm size have been successfully synthesized by wet chemical method in a water-ethylene glycol medium. The Co doping in ZnO resulted in decreasing the particle size and crystallinity while the increase in band gap.

EXPERIMENTAL

Analytical grade $ZnCl_2 \cdot 2H_2O$ and $CoCl_2 \cdot 6H_2O$ were used as starting materials for the synthesis of $Zn_{1-x}Co_xO$ series. In a typical synthesis procedure, citric acid was added to 100 mL of distilled water with magnetic stirring, until pH becomes 1.5. Required amounts of $ZnCl_2 \cdot 2H_2O$ and $CoCl_2 \cdot 6H_2O$ with

†Presented to the National Conference on Recent Advances in Condensed Matter Physics, Aligarh Muslim University, Aligarh, India (2011).

(x = 0 and 0.05) were added to the solution and dissolved. 10 mL of ethylene glycol was added to the above solution and stirred for 20 min. Sufficient amount of aqueous ammonia (15 mol/L) was added drop wise under magnetic stirring. The resulting solution was stirred for 0.5 h. Finally, a gel was obtained which was washed several times with water and ethanol. Gel was dried at 110 ºC for 12 h in an oven. The dried powder was further calcined at 400 ºC for 2 h resulting in the formation of Co-doped ZnO nanoparticles. Crystallinity, structure and crystallite size of Co-doped ZnO nanoparticles were determined by XRD (Rigaku) using Cu-K_α radiations (λ = 0.15406 nm) in 2θ range from 20º to 80º. SEM images were taken using FEI FESEM. High-resolution transmission electron microscopy (HRTEM) images were obtained using a (FE-TEM) (JEOL/JEM-2100F version) operated at 200 KV. The elemental composition was determined by energy dispersive X-ray spectroscopy (EDS, Inca Oxford). The samples were coated with a thin layer of gold to prevent charging of the samples. UV-Visible absorbance spectra have been recorded using Perkin-Elmer Lambda 35 UV/Vis spectrometer. Fourier transform infrared (FT-IR) spectra of the powders (as pellets in KBr) were recorded using a Fourier transform infrared spectrometer (Perkin Elmer) in the range of 4000-400 cm^{-1} with a resolution of 1 cm^{-1}.

RESULTS AND DISCUSSION

The typical XRD patterns of the pure and Co-doped ZnO samples annealed at 400 ºC are shown in Fig. 1. The peak positions of each sample exhibit the wurtzite structure of ZnO which were confirmed from the ICDD card No. 80-0075. Further, no other impurity peak was observed in the XRD pattern showing the single phase character of the sample. The crystallite size of both the samples were calculated using Scherrer formula[40], $D = \frac{0.9\lambda}{\beta\cos\theta}$, where λ is the wavelength of X-ray radiation, β is the full width at half maximum (FWHM) of the peaks at the diffracting angle θ. The calculated crystallite sizes of each sample are given in Table-1. It can be observed from Table-1 that the crystallite size of ZnO decreases from 27.1 to 21.3 nm when Co^{2+} content is increased from 0 to 5 %. The data revealed that the presence of Co^{2+} ions in ZnO prohibited the growth of crystal grains. The ionic radius of Co^{2+} is 58 pm whereas that of Zn^{2+} is 60 pm[41]. The Co ions substitute the Zn^{2+} ions in the crystal due to comparable ionic radius. However, the decrease in the lattice parameter may be due to the smaller ionic radii of Co^{2+} ions[42].

The XRD spectra have also been used to study the crystallinity of the samples. The doping of cobalt in ZnO not only lowers the particle size but also degrades the crystallinity of the nanoparticles. As the Co content increases, the intensity of XRD peaks decreases and FWHM increases (Fig. 1) which is due to the degradation of crystallinity. This means that even though the Co ions occupy the regular lattice site of Zn^{2+}, it produces crystal defects around the dopants and these defects change the stoichiometry of the materials.

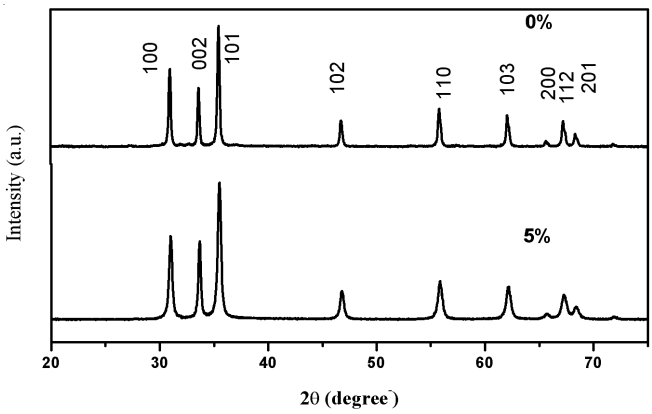

Fig. 1. XRD spectra of pure and cobalt doped ZnO nanoparticles

Fig. 2 shows the typical morphology of pure (Fig. 2a) and 5 % Co doped (Fig. 2b) ZnO nanoparticles and shows the presence of large spherical aggregates of smaller individual nanoparticles. Fig. 3 demonstrates transmission electron microscopy images taken for pure (Fig. 3a) and 5 % Co-doped (Fig. 3b) ZnO nanoparticles. It can be observed from the Fig. 3 that ZnO grains had a spherical morphology with an average diameter of 55 nm for pure ZnO, while 20 nm for 5 % Co-doped ZnO. Particle size obtained from TEM analysis is

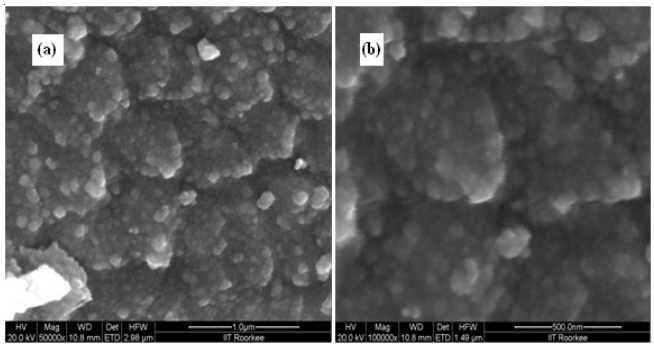

Fig. 2. SEM images of (a) pure and (b) 5 % cobalt doped nanoparticles

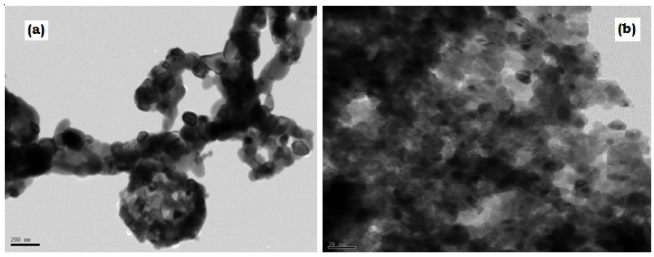

Fig. 3. TEM images of (a) pure and (b) 5 % cobalt doped nanoparticles

TABLE-1
VARIATION OF CRYSTALLITE SIZE, LATTICE PARAMETER, BAND GAP AND CELL VOLUME WITH DOPANT CONCENTRATION

Dopant concentration (%)	Crystallite size (nm)	Lattice parameter (a=b) (Å)	Lattice parameter (c) (Å)	Band gap (eV)	Cell volume (Å^3)
0	27.1	3.265	5.210	3.22	48.09
5	21.3	3.258	5.207	3.30	47.86

slightly greater than the crystallite calculated from XRD spectra. It may be due to the aggregation of nanoparticles during sample preparation for TEM analysis. Powder samples were dispersed in ethanol and sonicated in an ultrasonic bath for 15 min for TEM analysis. It is also clear from TEM results that Co doping in ZnO reduces the particle size.

Fig. 4 illustrates the EDAX spectra of elemental composition of pure (Fig. 4a) and 5 % Co doped (Fig. 4b) ZnO nanoparticles. The presence of Co is confirmed from the selective area EDAX analysis (Fig. 4). It can be verified from the results of XRD and EDAX that the Co is successfully doped in the ZnO nanocrystals.

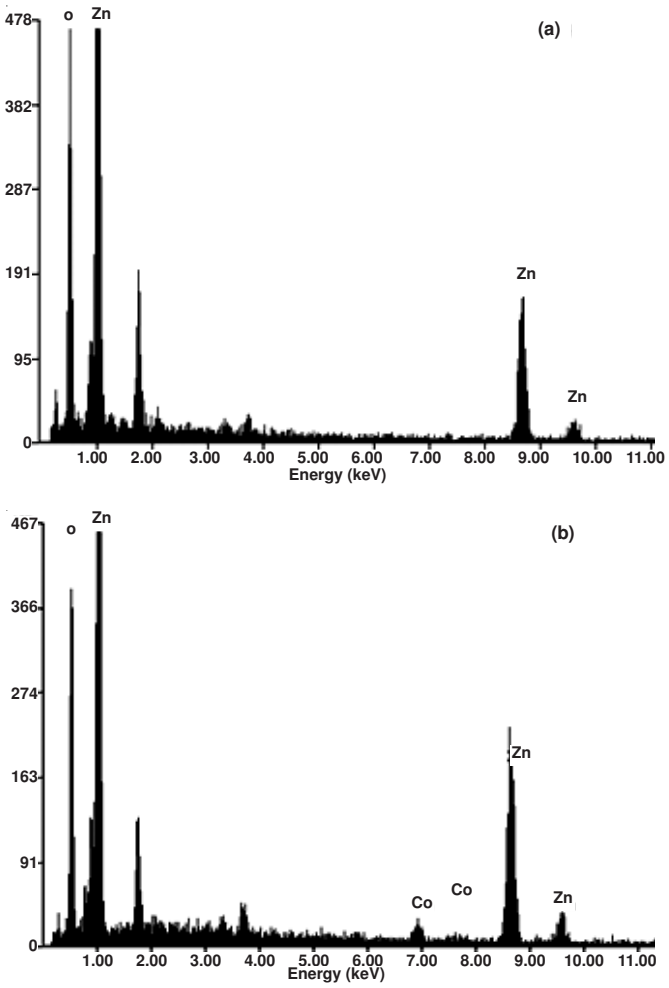

Fig. 4. EDAX images of (a) 0 % (b) 5 % Co doped ZnO nanoparticles

UV-visible absorption spectroscopy is a powerful technique to explore the optical properties of semiconducting nanoparticles. The optical absorption spectra of pure and Co doped ZnO nanoparticles are shown in Fig. 5. The absorbance is expected to depend on several factors, such as band gap, oxygen deficiency surface roughness and impurity centers[43]. Absorbance spectra exhibits an absorption edge at around 380-389 nm which can be attributed to the photo-excitation of electrons from valence band to conduction band. The absorption edge of pure and doped samples slightly varies as that of Co is introduced in the ZnO nanoparticles. The absorption edges of pure and 5 % Co doped ZnO are 386 and 376 nm, respectively. The position of the absorption spectra is observed to

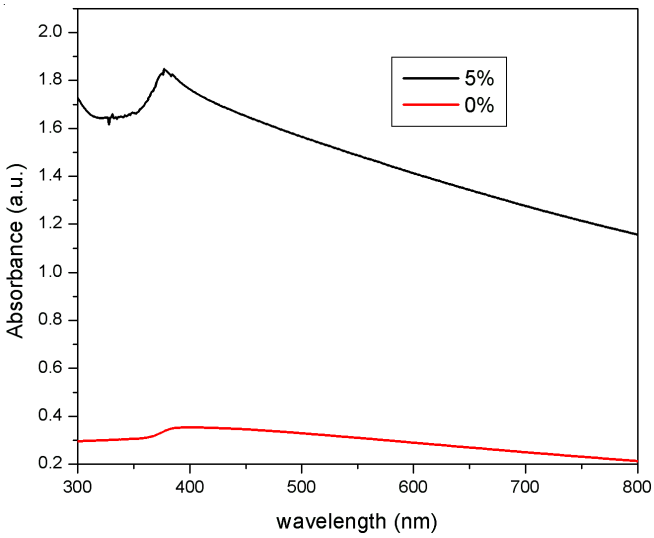

Fig. 5. Absorbance spectra of pure and cobalt doped ZnO nanoparticles

shift toward the lower wavelength side with increase in Co doping concentration in ZnO. This indicates that the band gap of ZnO material increases with the doping concentration of Co^{2+} ion. The increase in the band gap or blue shift can be explained on the basis of the Burstein-Moss effect[44]. When Fermi level shifts close to the conduction band due to the increase in the carrier concentration the low energy transitions are blocked and the value of band gap increases. The present experimental results are in good agreement with the results reported by Sakai *et al.*[45]. In order to verify the increase in band gap as discussed above, we have calculated the band gap using the Tauc relation[42].

$$\alpha h\nu = A(h\nu - E_g)^n$$

where α is the absorption coefficient, A is a constant and n = ½ for direct band gap semiconductor. An extrapolation of the linear region of a plot of $(\alpha h\nu)^2$ *vs.* $h\nu$ gives the value of the optical band gap E_g[43]. The measured band gaps are displayed in Table-1 shows a slight increase with the increase in dopant concentration. This is also in good agreement to the quantum confinement effect of the nanoparticles[46].

Fig. 6 shows the FTIR spectra of pure and Co-doped ZnO. FTIR spectra exhibit strong vibrations at around 630 and 430 cm^{-1} which are assigned to stretching (Co-O) and (Zn-O) respectively[47,48]. It is evident that the absorption band at around 3500 cm^{-1} in 3 % Co-doped sample is due to the hydroxyl stretching mode (OH) which may be due to moisture. The absorption peak at 2337 cm^{-1} is because of an existence of CO_2 molecule in air. A weak absorption peak at 1515 cm^{-1} is ascribed to (C=O). FTIR results confirm the formation of pure Co-doped ZnO samples as there is no vibration obtained from intermediate product.

Conclusion

Wet chemical synthesis route has been successfully used to synthesize Co-doped ZnO nanoparticles. The XRD patterns show that the prepared samples are wurtzite in structure with the size range of 21.3-27.1 nm. No impurity phase has been observed in XRD. The crystallinity, particle size and lattice constants are decreasing with the increase in cobalt concen-

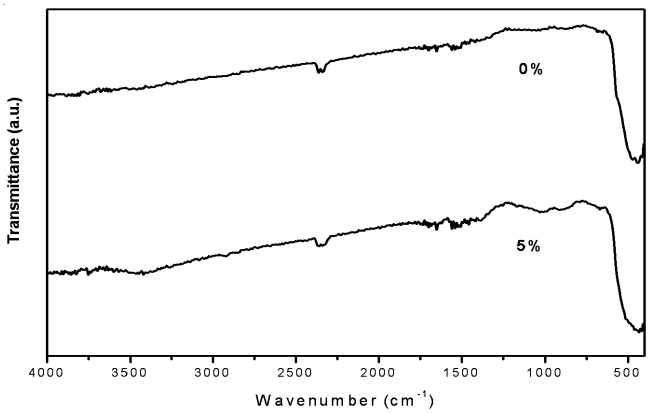

Fig. 6. FTIR spectra of pure and cobalt doped ZnO nanoparticles

tration. EDAX spectra confirm the existence of Co in doped samples. XRD, SEM and TEM results confirm the reduction in particle size with doping. The optical studies have been carried out using optical absorbance and FTIR spectroscopy. The band gap of the doped samples show a broadening effect as measured from the Tauc relation. Thus the cobalt doping can be used as an effective method for tailoring the optical and structural properties of ZnO nanoparticles.

ACKNOWLEDGEMENTS

The authors are grateful to the Council of Science & Technology (CST), Government of Uttar Pradesh, India for financial support in the form of Center of Excellence in Materials Science (Nano-materials). The authors are also thankful to the Head, School of Nano and Advanced Materials Engineering, Changwon National University, Republic of Korea for providing TEM and EDAX facility.

REFERENCES

1. S. Suwanboon, P. Amornpitoksuk, A. Haidoux and J.C. Tedenac, *J. Alloys Compd.*, **462**, 335 (2008).
2. P. Zu, Z.K. Tang, G.K.L. Wong, M. Kawasaki, A. Ohtomo, K. Koinuma and Y. Sagawa, *Solid State Commun.*, **103**, 459 (1997).
3. A.N. Gruzintsev, V.T. Volkov and E.E. Yakimov, *Semiconductors*, **37**, 259 (2003).
4. H. Hayashi, A. Ishizaka, M. Haemori and H. Koinuma, *Appl. Phys. Lett.*, **82**, 1365 (2003).
5. M. Liu, A.H. Kitai and P. Mascher, *J. Lumin.*, **54**, 35 (1992).
6. P. Sharma, K. Sreenivas and K.V. Rao, *J. Appl. Phys.*, **93**, 3963 (2003).
7. M.L. Curri, R. Comparelli, P.D. Cozzoli, G. Mascolo and A. Agostiano, *Mater. Sci. Eng. C*, **23**, 285 (2003).
8. H. Kim, J.S. Horwitz, W.H. Kim, A.J. Makinen, Z.H. Kafafi and D.B. Chrisey, *Thin Solid Films*, **420/421**, 539 (2002).
9. M. Ohtaki, T. Tsubota, K. Eguchi and H. Arai, *J. Appl. Phys.*, **79**, 1816 (1996).
10. T.R.N. Kutty and N. Raghu, *Appl. Phys. Lett.*, **54**, 1796 (1989).
11. M. Chen, Z.L. Pei, C. Sun, J. Gong, R.F. Huang and L.S. Wen, *Mater. Sci. Eng. B*, **85**, 212 (2001).
12. J. Lee, H. Lee, S. Seo and J. Park, *Thin Solid Films*, **398/399**, 641 (2001).
13. T. Dietl, H. Ohno and F. Matsukura, *Phys. Rev. B*, **63**, 195205 (2001).
14. Y. Uspenski, E. Kulatov, H. Mariette, H. Nakayama and H. Ohta, *J. Magn. Magn. Mater.*, **258/259**, 248 (2003).
15. K. Sato and H. Katayama-Yoshida, *Physica B*, **308**, 904 (2001).
16. K. Sato and H. Katayama-Yoshida, *Phys. Status Solid. B*, **229**, 673 (2002).
17. K. Sato and H. Katayama-Yoshida, *Semicond. Sci. Technol.*, **17**, 367 (2002).
18. A.F. Jalbout, H. Chen and S.L. Whittenburg, *Appl. Phys. Lett.*, **81**, 2217 (2002).
19. K. Ando, H. Saito, Z. Jin, T. Fukumura, M. Kawasaki, Y. Matsumoto and H. Koinuma, *Appl. Phys. Lett.*, **78**, 2700 (2001).
20. T. Makino, Y. Segawa, M. Kawasaki, A. Ohtomo, R. Shiroki, K. Tamura, T. Yasuda and H. Koinuma, *Appl. Phys. Lett.*, **78**, 1237 (2001).
21. N. Lebedeva and P. Kuivalainen, *J. Appl. Phys.*, **93**, 9845 (2003).
22. K. Ando, H. Saito, Z. Jin, T. Fukumura, M. Kawasaki, Y. Matsumoto and H. Koinuma, *J. Appl. Phys.*, **89**, 7284 (2001).
23. K. Ando, H. Saito, Z. Jin, T. Fukumura, M. Kawasaki, Y. Matsumoto and H. Koinuma, *Appl. Phys. Lett.*, **78**, 2700 (2001).
24. T. Sehili, P. Boule and J. Lemaire, *J. Photochem. Photobiol. A*, **50**, 103 (1989).
25. J. Villasenor, P. Reyes and G. Pecchi, *J. Chem. Technol. Biotechnol.*, **72**, 105 (1998).
26. M.D. Driessen, T.M. Miller and V.H. Grassian, *J. Molecul. Catal. A*, **131**, 149 (1998).
27. I. Djerdj, J. Zvonko, A. Denis and N. Markus, *Nanoscale*, **2**, 1096 (2010).
28. I. Djerdj, G. Garnweitner, D. Arcon, M. Pregelj, Z. Jaglicic' and M. Niederberger, *J. Mater. Chem.*, **18**, 5208 (2008).
29. H.K. Park, D.K. Kim and C.H. Kim, *J. Am. Ceram. Soc.*, **80**, 743 (1997).
30. S.I. Hirano, *Ceram. Bull.*, **66**, 1342 (1987).
31. D. Vorkapic and T. Matsoukas, *J. Am. Ceram. Soc.*, **81**, 2815 (1998).
32. Y.X. Li and K.J. Klabunde, *Chem. Mater.*, **4**, 611 (1992).
33. V.R. Palkar, *Nanostruct. Mater.*, **11**, 369 (1999).
34. C.G. Granqvist and R.A. Burhman, *J. Appl. Phys.*, **47**, 2200 (1976).
35. T.T. Kodas, *Adv. Mater.*, **6**, 180 (1989).
36. G.L. Messing, S.C. Zhang and G.V. Jayanthi, *J. Am. Ceram. Soc.*, **76**, 2707 (1993).
37. P.P. Sahay, S. Tewari and R.K. Nath, *Cryst. Res. Technol.*, **42**, 723 (2007).
38. G.D. Ulrich and J.W. Riehl, *J. Colloid. Interf. Sci.*, **87**, 257 (1982).
39. G. Skanadan, Y.J. Chen, N. Glumac and B.H. Kear, *Nanostruct. Mater.*, **11**, 149 (1999).
40. A.L. Patterson, *Phys. Rev.*, **56**, 978 (1939).
41. X. Wang, R. Zheng, Z. Liu, Ho-Pui Ho, J. Xu and S.P. Ringer, *Nanotechnology*, **19**, 455702 (2008).
42. S. Suwanboon, P. Amornpitoksuk, A. Haidoux and J.C. Tedenac, *J. Alloys Compd.*, **462**, 335 (2008).
43. A. Azam, A.S. Ahmed, M.S. Ansari, M. Shafeeq and A.H. Naqvi, *J. Alloys Compd.*, **506**, 237 (2010).
44. S. Suwanboon, T. Ratana and W.T. Ratana, *J. Sci. Technol.*, **4**, 111 (2007).
45. K. Sakai, T. Kakeno, T. Ikari, S. Shirakata, T. Sakemi, K. Awai and T. Yamamoto, *J. Appl. Phys.*, **99**, 043508 (2006).
46. T. Takagahara and K. Takeda, *Phys. Rev. B*, **46**, 15578 (1992).
47. R. Fu,W. Wang, R. Han and K. Chen, *Mater. Lett.*, **62**, 4066 (2008).
48. Y.Y. Hong, S.Z. Zhang, G.Q. Di, H.Z. Li, Y. Zheng, J. Ding and D.G. Wei, *Mater. Res. Bull.*, **43**, 2457 (2008).